Mechanism of Cholera Toxin Action on a Polarized Human Intestinal Epithelial Cell Line: Role of Vesicular Traffic

Wayne I. Lencer,*‡‖ Charlene Delp,§ Marian R. Neutra,‡‖ and James L. Madara§‖

*Combined Program in Pediatric Gastroenterology and Nutrition and ‡GI Cell Biology Laboratory, The Children's Hospital; §Department of Pathology, Brigham's and Women's Hospital; and ‖Departments of Pediatrics and Pathology, Harvard Medical School, Boston, Massachusetts 02115

Abstract. The massive secretion of salt and water in cholera-induced diarrhea involves binding of cholera toxin (CT) to ganglioside GM1 in the apical membrane of intestinal epithelial cells, translocation of the enzymatically active A_1-peptide across the membrane, and subsequent activation of adenylate cyclase located on the cytoplasmic surface of the basolateral membrane. Studies on nonpolarized cells show that CT is internalized by receptor-mediated endocytosis, and that the A_1-subunit may remain membrane associated. To test the hypothesis that toxin action in polarized cells may involve intracellular movement of toxin-containing membranes, monolayers of the polarized intestinal epithelial cell line T84 were mounted in modified Ussing chambers and the response to CT was examined. Apical CT at 37°C elicited a short circuit current (Isc: 48 ± 2.1 $\mu A/cm^2$; half-maximal effective dose, ED50 ~0.5 nM) after a lag of 33 ± 2 min which bidirectional $^{22}Na^+$ and $^{36}Cl^-$ flux studies showed to be due to electrogenic Cl^- secretion. The time course of the CT-induced Isc response paralleled the time course of cAMP generation. The dose response to basolateral toxin at 37°C was identical to that of apical CT but lag times (24 ± 2 min) and initial rates were significantly less. At 20°C, the Isc response to apical CT was more strongly inhibited (30–50%) than the response to basolateral CT, even though translocation occurred in both cases as evidenced by the formation of A_1-peptide. A functional rhodamine-labeled CT-analogue applied apically or basolaterally at 20°C was visualized only within endocytic vesicles close to apical or basolateral membranes, whereas movement into deeper apical structures was detected at 37°C. At 15°C, in contrast, reduction to the A_1-peptide was completely inhibited and both apical and basolateral CT failed to stimulate Isc although Isc responses to 1 nM vasoactive intestinal peptide, 10 μM forskolin, and 3 mM 8Br-cAMP were intact. Re-warming above 32°C restored CT-induced Isc. Preincubating monolayers for 30 min at 37°C before cooling to 15°C overcame the temperature block of basolateral CT but the response to apical toxin remained completely inhibited. These results identify a temperature-sensitive step essential to apical toxin action on polarized epithelial cells. We suggest that this event involves vesicular transport of toxin-containing membranes beyond the apical endosomal compartment.

COLONIZATION of the small intestine by *V. Cholerae* results in diarrhea due to massive salt and water secretion without epithelial damage (12). The primary transport event of secretory diarrhea, electrogenic Cl^- secretion (24), is induced in part by the direct action of cholera toxin (CT)[1] on polarized intestinal epithelial cells and is mediated by an increase in intracellular cAMP generated by adenylate cyclase (7, 36, 52, 58).

CT (86 kD) consists of five identical B-subunits (11.6 kD) that bind specifically to ganglioside GM_1 on cell membranes, and a single enzymatic A-subunit (27 kD). The A-subunit is comprised to two peptides (23 and 5 kD) linked by extensive noncovalent interactions and a single disulfide bond (60). Studies on a variety of intact nonpolarized cells have established that CT activates adenylate cyclase through a complex chain of events. Binding of the B-subunits to ganglioside GM_1 on the cell surface (8, 17, 27) is followed by translocation of the A-subunit across the membrane (35, 56, 67) and reduction of the disulfide bond to form the enzymatically active A_1-peptide. The reduced A_1-peptide functions inside the cell, catalyzing the ADP-ribosylation of the regulatory GTPase $G_{\alpha s}$ that in turn activates adenylate cyclase (6, 20, 33, 48). Even in cells with abundant receptors, cAMP accumulation in the cytoplasm is not detected until at least 10 min after CT binds to the cell surface (3, 15). This lag

1. *Abbreviation used in this paper*: CT, cholera toxin.

phase has been thought to represent the time required for A_1 to cross the plasma membrane and interact with $G_{\alpha s}$ on the cytoplasmic face of the membrane (16, 22, 67). In nonpolarized cells, the CT-receptor (GM_1), $G_{\alpha s}$, and the adenylate cyclase complex are located on the same plasma membrane domain.

In nature, however, CT makes initial contact with GM_1 in the apical membrane of polarized intestinal epithelial cells and subsequently activates adenylate cyclase that is located on the cytoplasmic surface of the basolateral membrane (10, 11, 49, 50, 54, 64). Thus, the site of toxin binding is separated from the target enzyme by circumferential tight junctions. Since neither extracellular CT nor intramembrane GM_1 can pass through tight junctions (53, 62), it has been assumed that after binding, the A-subunit of the toxin gains access to $G_{\alpha s}$, and possibly to the basolateral membrane and adenylate cyclase, by penetrating the apical plasma membrane, dissociating from the B-subunit, and moving across the cell by an undefined route. Even in nonpolarized cells, however, the events that follow binding of CT at the cell surface and lead to activation of adenylate cyclase are not entirely clear. Although it is agreed that the toxin's enzymatic A-subunit penetrates the plasma or possibly the endosomal membrane (31), the idea that the A_1-peptide breaks free of the membrane and diffuses in the cytoplasm has been questioned (32, 35). Indeed, several lines of evidence indicate that the A_1-peptide remains membrane associated after translocation (22, 23, 65).

CT is internalized by receptor-mediated endocytosis in nonpolarized cells (16, 34, 46). Recent data from hepatocytes suggest that endocytosis and subsequent traffic of toxin-containing membranes may be involved in facilitating interactions between the A_1-peptide, $G_{\alpha s}$, and adenylate cyclase (31, 32). Intestinal enterocytes in vivo were shown to conduct both endocytosis and transepithelial transport of CT (25). Thus, if the A_1-peptide remains membrane associated, the toxin could be carried to its site of action in polarized cells by vesicular transport. An alternative hypothesis, based on the ability of CT to ribosylate $G_{\alpha s}$ in brush border membranes isolated from rabbit intestine, proposes that it is not CT, but rather ADP-ribose-$G_{\alpha s}$ that moves across the cell to activate adenylate cyclase at the basolateral membrane (10, 11).

The purpose of this study was to test the hypothesis that endocytosis and vesicular transport are required for the action of CT on polarized intestinal epithelial cells. We used a human intestinal cell line, T84, which forms confluent monolayers of polarized columnar cells that display features of intestinal crypt cells. T84 cell monolayers respond to cAMP agonists with electrogenic Cl^- secretion and thus are suitable models to study regulatory mechanisms of intestinal salt and water secretion (9). The monolayers were grown on permeable supports that allowed experimental access to both apical and basolateral cell surfaces. We found that when applied to either apical or basolateral cell surfaces of T84 cell monolayers, CT induced a cAMP-dependent Cl^- secretory response analogous to that seen in intact intestine. The ability of apical CT to elicit Cl^- secretion, however, involved a temperature-sensitive step that was not necessary for the action of basolateral CT. Our data provide strong evidence in support of a role for vesicular transport in the mechanism of CT action on polarized epithelial cells.

Materials and Methods

Materials

CT was obtained from Calbiochem-Behring Corp. (San Diego, CA), Na ^{125}Iodine from New England Nuclear (Boston, MA), and 5-(and-6)-carboxytetramethylrhodamine and its succinimidyl ester from Molecular Probes, Inc. (Eugene OR). All other reagents unless otherwise stated were from Sigma Chemical Co. (St. Louis, MO). Mammalian Ringer's solution (114 mM NaCl, 5 mM KCl, 1.65 mM Na_2HPO_4, 0.3 mM NaH_2PO_4, 25 mM $NaHCO_3$, 1.1 mM $MgSO_4$, 1.25 mM $CaCl_2$ to which 10 mM glucose was added) was used for all assays in Ussing chambers. HBSS (containing in g/liter 0.185 $CaCl_2$, 0.098 $MgSO_4$, 0.4 KCl, 0.06 KH_2PO_4, 8 NaCl, 0.048 Na_2HPO_4, 1 glucose, to which was added 10 mM Hepes, pH 7.4) was used for micro-assay of Cl^- secretion, measurement of A_1-peptide formation, and morphologic studies.

Cell Culture

T84 cells obtained from ATCC were cultured and passaged as previously described (9) in equal parts of DME 1 g/l D-glucose) and Ham's F-12 Nutrient mixture, supplemented with 5% newborn calf serum, 15 mM Hepes, 14 mM $NaHCO_3$, 40 mg/liter penicillin, 8 mg/liter ampicillin, and 0.90 mg/liter streptomycin. Cells were seeded at confluent density onto rat tail collagen-coated Nucleopore filters (9) glued to 2-cm^2 Lexan rings or 0.33-cm^2 Transwell inserts (Costar Laboratories, Cambridge, MA) coated with a dilute collagen solution as previously described (43). Transepithelial resistances attained stable levels (>1,000 ohms·cm^2) after 7 d. The development of high transepithelial resistance correlated with the formation of confluent monolayers with well-developed tight junctions as assessed by morphological analysis (42), and with the ability of monolayers to secrete Cl^-. Cells from passages 61 to 85 were utilized for these experiments.

Electrophysiology and Bidirectional Flux Studies

For electrophysiological studies, confluent monolayers were transferred to mammalian Ringers solution or HBSS. Measurements of short circuit current (Isc) and resistance (R) were performed either with 2 cm^2 or 0.33 cm^2 monolayers as previously described (9, 43). Briefly, serosal and mucosal reservoirs were interfaced with calomel and Ag-AgCl electrodes via 5% agar bridges made with Ringers buffer. Measurements of resistance were made using a dual voltage clamp device (University of Iowa) and 100 or 25 μA current pulses. For measurements made on 0.33 cm^2 monolayers, short circuit current (Isc) was calculated using Ohm's law.

Bidirectional fluxes of ^{22}Na and ^{36}Cl were performed in Ussing chambers under short circuit conditions using 2 cm^2 monolayers as previously described (47). Monolayers were matched for baseline resistance such that differences in resistance were <20%. After monolayers were mounted, trace quantities of ^{22}Na and ^{36}Cl were added to mucosal or serosal reservoirs of matched monolayers. After an equilibration period, 120 nM CT was added to apical chambers. Two 15-min baseline periods during the lag phase (before CT-induced Cl^- secretion) and two 15-min periods in the secretory phase were studied.

Measurement of CT-induced cAMP Levels

Measurements of cAMP were performed on ethanol extracts of T84 monolayers (2 cm^2 rings) exposed apically to 120 nM CT in HBSS at 37°C for various intervals ranging from 0 to 75 min. The incubations were stopped by immersion into HBSS at 4°C, and extracting the cell contents into 0.7 ml 66% ethanol/Ringers (vol/vol). Radioimmunoassay kits were used to measure cell-associated cAMP as directed by the supplier (New England Nuclear).

Quantitation of Cell-specific Reduction of A-Subunit after Binding of CT to T84 Cells

CT-^{125}I was prepared as previously described (38) and had a specific activity of 100–400 cpm/fmol and a half-maximal effective dose (ED50) identical to that of native toxin when applied to apical surfaces of T84 monolayers. Reduction of the A-subunit to the A_1-peptide was assessed using modifications of methods described by Kassis (35). T84 monolayers (2-cm^2 rings) were incubated with 120 nM ^{125}I-CT in HBSS applied apically at 4°, 15°, and 20°C for 2 h, and at 37°C for 30 min or 1 h. Incubations were stopped by immersion into HBSS containing 10 mM N-ethylmale-

imide (Calbiochem-Behring Corp.) at 4°C for at least 15 min, followed by treatment with 2.5 μM diisopropylfluorophosphate. The rings were placed on a drop of silica grease on a glass plate cooled to 4°C. Total cell extracts were made by scraping the cells into 100 μl lysis buffer (2% Triton-X 100, 10 mM Hepes, 3.5 mM $MgCl_2$, 1 mM PMSF, 10 μg/ml chymostatin, and 2 mM N-ethylmaleimide, pH 7.4), vortexing vigorously, then clarifying by centrifugation for 3 min at 14,000 RPM in an Eppendorf microfuge. The extracts were diluted 1:1 in 2× sample buffer and run on nonreducing 12.5% SDS-polyacrylamide gels. The gels were stained and fixed with Coomassie blue, destained, and each lane was cut into 1-mm slices. Total radioactivity in slices was quantified by gamma counting, and radioactive peaks corresponding to A-, A_1-, and B-subunits were identified. The fractional component of A_1-peptide was defined as the ratio of A_1- to A-band integrals.

Epifluorescence Microscopy of CT Binding and Internalization

To prepare rhodamine-labeled CT, 1 mg of the lyophilized toxin was reconstituted with 200 μl of 25 mM sodium carbonate, pH 9.2, and immediately incubated at 21°C for 1 h with 0.1 mg tetramethylrhodamine succidimal ester freshly dissolved in N,N-dimethylformamide. The reaction mixture was passed over a Sephadex G-25 (Pharmacia, Upsalla, Sweden) column equilibrated with a solution containing 130 mM NaCl and 20 mM Tris, pH 7.5. The first three 0.5-ml fractions of the void volume were collected and pooled. Concentration of toxin in these fractions was determined by absorbance at 280 nm using an extinction coefficient $A^{1\%}_{1cm}$ = 11.42 (39). The molar ratio of rhodamine to CT was determined by comparison of a 0.1% pronase (Boehringer Mannheim Biochemicals, Indianapolis, IN) digest of the rhodamine-labeled CT analogue (CT-rhod) to a 1-mg/ml standard solution of 5-(and-6)-carboxytetramethylrhodamine in an SLM 8000 fluorimeter (Urbana, IL). The toxin was labeled with rhodamine in a ratio of 1:2.4.

After incubation with 20 mM CT-rhod, T84 monolayers were washed three times in HBSS at 4°C and fixed in 4% paraformaldehyde in PBS (150 mM NaCl, and 20 mM NaH_2PO_4/Na_2HPO_4, pH 7.4) overnight. Fixed monolayers were cryoprotected by incubation in 30% sucrose (wt/vol) in PBS for at least 2 h. The monolayers on their filter supports were cut from the lexan rings, sliced into strips, stacked together in Cryoform embedding medium (International Equipment Co., Needham, MA) in perpendicular orientation on copper blocks, and frozen by immersion in liquid nitrogen. 5-μm frozen sections were cut on a IECMinotome microtome cryostat (Needham, MA), picked up on glass slides previously coated with 2% 3 aminopropyl-triethoxy-silane in acetone, mounted in 1:1 PBS/glycerol containing 1% n-propyl gallate or in Moviol (Hoechst, Switzerland) and examined using a Zeiss Axiophot photomicroscope (W. Germany) equipped with a 546 ± 12-nm narrow band pass excitation filter and a 590-nm-long pass barrier filter. Photographs were taken using T-Max 400 film (Eastman Kodak Co., Rochester, NY).

Statistics

Bidirectional flux studies, and temperature effects on formation of A_1-peptide lag phase and dIsc/dt were analyzed by ANOVA, or T-test using Statview 512+ software (Brainpower, Inc., Calabasas, CA).

Results

Polarized T84 Cells Respond to CT with cAMP-dependent Cl^- Secretion

Initial studies were performed to define T84 cells as a model to study the mechanism of CT action on polarized epithelia. To this end, we applied CT apically to T84 monolayers mounted in modified Ussing chambers at 37°C. CT induced a dose-dependent increase in short circuit current (Isc) (Fig. 1). 120 nM CT elicited a maximal Isc response after a lag of 33 ± 2 min (mean ± SE, n = 3) and this dose was utilized throughout the study unless otherwise stated.

To identify the source of the CT-elicited Isc, bidirectional $^{22}Na^+$ and $^{36}Cl^-$ flux studies were performed under short circuit conditions on monolayers exposed apically to CT. Two

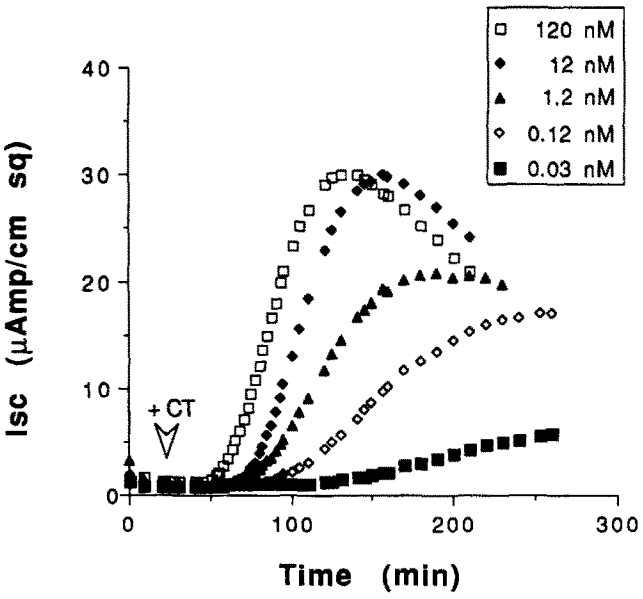

Figure 1. Time course and dose response of CT-induced change in Isc in T84 monolayers exposed apically to CT at 37°C. CT applied to the apical membrane elicits a dose-dependent response in T84 cells.

15-min periods during the lag phase and two 15-min periods during the secretory phase were studied. Fig. 2 shows data from a representative pair of T84 monolayers closely matched for transepithelial resistance, and Table I summarizes data from 14 independent samples. CT induced a 45 ± 5-fold increase in net serosal to mucosal Cl^- flux that accounted for 70 ± 10% (mean ± SD) of the CT-induced Isc. CT had no significant effect on serosal to mucosal Na^+ transport under short-circuit conditions indicating that the Cl^- secretory response did not influence tight junction permeability. The

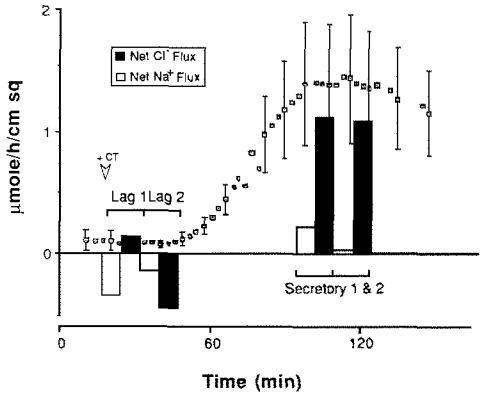

Figure 2. Net transepithelial flux of $^{36}Cl^-$ (*solid bars*) and $^{22}Na^+$ (*open bars*) in two independent T84 monolayers closely matched for transepithelial resistance. At the open arrowhead, 120 nM CT was applied to apical reservoirs at 37°C and the time course of CT-induced increase in Isc was measured (*open squares*). Flux measurements were made on two 15-min periods during the lag phase and on two 15-min periods during the secretory phase. Positive values represent secretion and negative values represent absorption. Cl^- secretion accounts fully for the CT-induced increase in Isc.

*Table I. Unidirectional Na^+ and Cl^- Fluxes**

Period	J^{Na}_{m-s}	J^{Na}_{s-m}	J^{Na}_{net}	J^{Cl}_{m-s}	J^{Cl}_{s-m}	J^{Cl}_{net}	Isc	R
	μeq/h/cm²	*μeq/h/cm²*	*μeq/h/cm²*	*μeq/h/cm²*	*μeq/h/cm²*	*μeq/h/cm²*	*μeq/h/cm²*	*ohms·cm²*
Lag 1	0.37 ± 0.05	0.31 ± 0.04	0.06 ± 0.03	0.33 ± 0.08	0.35 ± 0.04	−0.02 ± 0.03	0.09 ± 0.01	
Lag 2	0.38 ± 0.05	0.42 ± 0.02	−0.05 ± 0.05	0.42 ± 0.09	0.46 ± 0.02	−0.04 ± 0.08	0.10 ± 0.01	1430 ± 69
Secretory 1	0.30 ± 0.04	0.48 ± 0.04	−0.18 ± 0.03	0.67 ± 0.08	1.6 ± 0.1	−0.9 ± 0.1‡	1.3 ± 0.15‡	
Secretory 2	0.35 ± 0.04	0.36 ± 0.05	−0.01 ± 0.06	0.76 ± 0.07	1.4 ± 0.2	−0.6 ± 0.1‡	1.3 ± 0.15‡	970 ± 60

* Unidirectional ion fluxes (*J*) mucosal to serosal (*m-s*) and serosal to mucosal (*s-m*), shortcircuit currents (*Isc*), and transepithelial resistances (*R*) are expressed as mean ± se microequivalents (*μeq*)/h/cm² of seven paired monolayers. Two 15-min periods during the lag phase (*lag 1 and 2*) and two 15-min periods during the secretory phase (*Secretory 1 and 2*) were studied.
‡ Indicates that values are significantly different from both control lag periods 1 and 2 by ANOVA ($P < 0.05$).

modest drop in transepithelial resistance during CT-induced Cl^- secretion can be fully accounted for by activation of ion channels in apical and basolateral membranes. With resistances greater than 400 ohms·cm², the paracellular flux of inulin (5 kD) and mannitol (182 D) is <5 nmol/h/cm² and 50 nmol/h/cm², respectively (42). In our studies, electrical resistances were continuously monitored and were always above 600 ohms·cm² at maximal secretion. The data are in agreement with previously published analyses of the effects of cAMP agonists on tight junction permeability (57).

To demonstrate that the CT-induced Cl^- secretion was mediated by activation of adenylate cyclase, the time course of toxin-induced cAMP production was examined. Fig. 3 shows that the onset of Cl^- secretion correlated closely with the time course of a CT-induced 74 ± 1-fold increase in cAMP. Taken together, these results define T84 cells as a valid model for the study of CT-induced Cl^- secretion in polarized epithelia.

T84 Cell Polarity Influences the Cl^- Secretory Response to Cholera Toxin

To examine the role of cell polarity in the response of T84 cells to CT, we first studied the dose response and time course of CT-induced Cl^- secretion after applying CT to either apical or basolateral surfaces of T84 cells. To compensate for the diffusion barrier presented by the collagen-coated filter at the basolateral cell surface, monolayers were routinely preincubated with CT at 4°C for 30–60 min before warming the system to 37°C. Previous studies have shown that, under the conditions used in these experiments, molecules as large as immunoglobulins have free access to basolateral cell membranes when applied to the serosal reservoir (51). Fig. 4 shows that the toxin induced an increase in Isc when applied either to apical or basolateral cell surfaces, and that the dose responses to apical and basolateral CT were nearly identical with an apparent half maximal effective dose (ED50) of ~0.5 nM. This agrees closely with the binding affinity of CT to brush border membranes prepared from rat intestine (38). The data indicate that apical and basolateral membranes of T84 cells contain similar numbers of functional CT receptors.

Differences were observed, however, in the time course of toxin action. When CT was applied to apical surfaces at 4°C and cells were warmed to 37°C (Fig. 5 *a*), CT induced a strong Cl^- secretory response after a lag of 33 ± 2 min (mean ± SE, $n = 6$). In contrast, when applied to basolateral surfaces, the CT-induced secretory response occurred

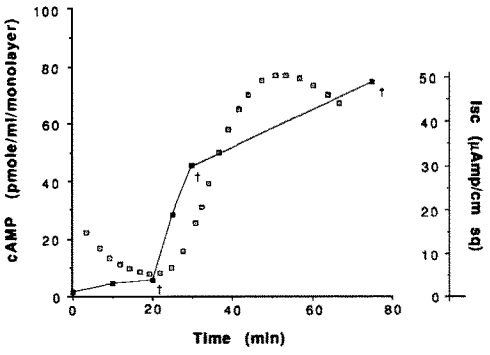

Figure 3. Time course of the cAMP response to apical CT at 37°C (*filled squares*). The secretory response to apical CT is also shown (*Isc, open squares*). Indicated points (†) are the mean of two or three independent measures. cAMP production parallels the Cl^- secretory response.

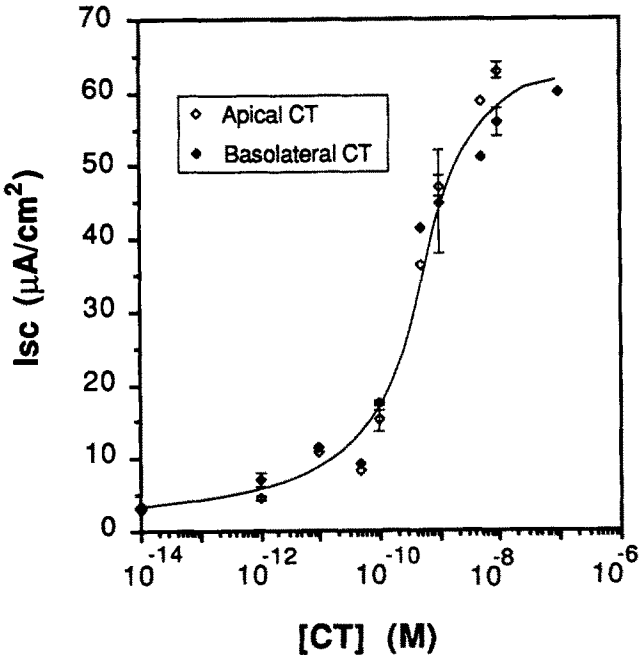

Figure 4. Dose response to CT applied apically (*open diamonds*) or basolaterally (*filled diamonds*) at 4°C for 30 min before warming to 37°C for 150 min. The dose dependency of apical and basolateral CT are nearly identical.

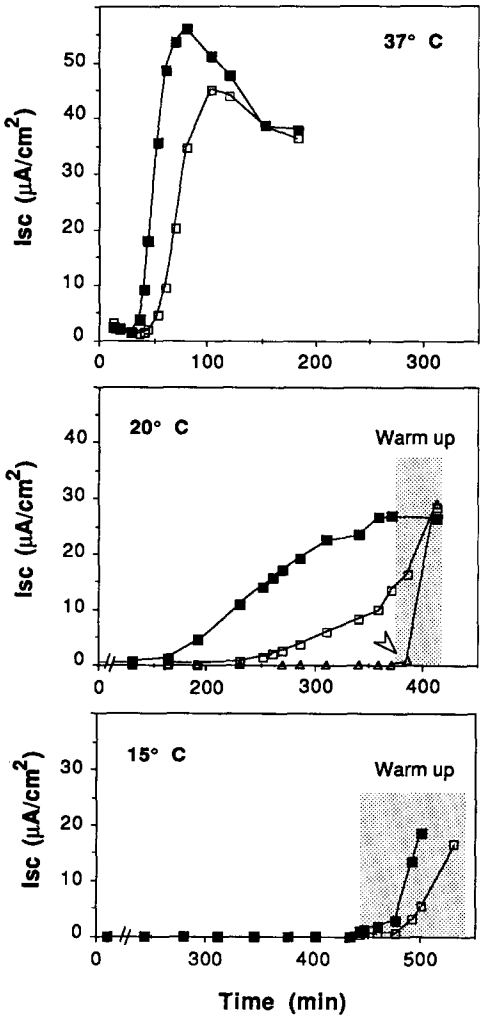

Figure 5. Temperature effect on the time course of change in Isc after apical (*open squares*) or basolateral (*filled squares*) application of CT. For comparison and visual clarity the curves are plotted on identical time scales, but only the time periods in which responses occur are shown. Shaded areas indicate periods when the monolayers were warmed to 32°C. Data from a control monolayer not exposed to CT is shown in the 20°C panel (*open triangles*). To demonstrate the viability of this control, 0.5 mM 8Br-cAMP was administered to the serosal reservoir at 385 min (*open arrowhead*). At 37°C, the action of apical CT in comparison to basolateral CT was both delayed and slower than that of basolateral toxin. At 20°C, the action of apical CT was disproportionately inhibited. At 15°C the action of both apical and basolateral toxin was completely blocked.

after a lag time of only 24 ± 2 min (2 tail *t* test, $P = 0.009$). In addition, initial rates of toxin-induced Cl^- secretion (dIsc/dt) were slower for apical toxin (1.23 ± 0.06 μA/cm²/min) than for basolateral toxin (2.0 ± 0.14 μA/cm²/min) ($P = 0.0005$). The peak secretory responses were similar, however, as evidenced by peak Isc of 48 ± 2.1 and 53 ± 3.3 μA/cm² after apical and basolateral CT, respectively. The data (summarized in Table II, 37°C) demonstrate that CT elicited a Cl^- secretory response of equal magnitude from T84 cells when exposed to either the apical or basolateral membrane at 37°C, but the onset of the secretory response due to apical toxin was significantly delayed and the initial rate was significantly slower.

Temperatures of 20°C or below are known to greatly impede budding, movement and/or fusion of membrane vesicles in the exocytic (30, 44), endosome-lysosome (13), and transcytotic pathways (5, 26). To examine whether a requirement for vesicular membrane transport might account for the apparent delay in apical toxin action at 37°C, we determined the effect of lowered temperature on CT-induced Cl^- secretion after exposure to apical or basolateral cell surfaces. T84 cell monolayers were preincubated with CT either apically or basolaterally at 4°C for 30–60 min, and then warmed to 15°, 20°, or 37°C. Fig. 5 shows data from a representative series of experiments. At 37°C (Fig. 5 *a*), the time course of toxin-induced Cl^- secretion in monolayers exposed to apical CT was delayed, with a slower rate of activation when

Table II. Temperature Dependency of Apical and Basolateral Toxin Action

Incubation temperature	37°C Preincubation	Toxin application	Baseline Isc	Peak Isc	Warm up	dIsc/dt	Lag phase	Relative dIsc/dt (apical/basolateral)	Relative lag (apical/basolateral)
			μA/cm²	*μA/cm²*	*μA/cm²*	*μA/cm²/m*	*min*		
37°C	none	Apical	3.0 ± 1.1	48 ± 2.1	–	1.23 ± 0.06	33 ± 2.0	0.64 ± 0.09	1.4 ± 0.08
n = 6 pairs		Basolateral	4.0 ± 1.4	53 ± 3.3	–	2.0 ± 0.14	24 ± 2.0		
20°C	none	Apical	0.4 ± 0.04	1.4 ± 0.15*	22 ± 3.2	0.048 ± 0.006	251 ± 9.0	0.39 ± 0.04‡	1.69 ± 0.04‡
n = 10 pairs		Basolateral	0.5 ± 0.05	11 ± 1.4*	22 ± 2.4	0.12 ± 0.012	149 ± 7.8		
15°C	none	Apical	0.4 ± 0.3	0.1 ± 0.00	17 ± 1	not present	not present	–	–
n = 3 pairs		Basolateral	0.2 ± 0.3	0.3 ± 0.08	13 ± 2	not present	not present		
15°	25 min	Apical	0.2 ± 0.05	0.5 ± 0.05	13 ± 1.4	not present	not present	complete	complete
n = 7 pairs		Basolateral	0.4 ± 0.06	9.3 ± 1.0	13 ± 1.7	0.035 ± 0.005	105 ± 5.5	apical block	apical block

* Monolayers exposed to apical CT at 20°C did not reach steady-state secretion within the 400-min period of observation. Therefore peak Isc at 20°C is arbitrarily reported 120 min after basolateral monolayers began secreting.
‡ Two-tail T-test $P < 0.04$.

compared to that of monolayers exposed to basolateral CT, as discussed above. At 20°C (Fig. 5 *b*), toxin-induced Cl^- secretion in response to both apical and basolateral CT was attenuated, but the time course of Cl^- secretion due to apical toxin was more strongly inhibited than that of basolateral toxin. In monolayers exposed to apical CT, lag times were disproportionately longer (275 vs 170 min) and initial rates were disproportionately slower (0.06 vs. 0.12 $\mu A/cm^2/m$). Table II (20°C) summarizes the results of 10 independent experiments. Lag times at 20°C for apical and basolateral toxin were 251 ± 9 and 149 ± 8 min and initial rates were 0.048 ± 0.006 and 0.12 ± 0.01 $\mu A/cm^2/min$, respectively (mean ± SE). Re-warming the monolayers above 32°C (Fig. 5 *b*, *shaded area*) showed that the cells responded equally to apical or basolateral CT (peak Isc: 22 ± 3.2 and 22 ± 2.4 $\mu A/cm^2$, n = 10). Re-warming, however, did not influence Cl^- secretion in control monolayers not exposed to CT. To confirm the viability of these nonexposed controls, 0.5 mM 8B4-cAMP was administered to basolateral reservoirs of control monolayers (Fig. 5 *b*, *arrowhead*), and this was followed by an immediate rise in Isc (peak Isc: 20 ± 3.8 $\mu A/cm^2$, dIsc/dt: 1.1 ± 0.16 $\mu A/cm^2/min$, n = 7). To quantitate the differential effect of temperature on the time course of apical and basolateral toxin action, relative lag times and relative rates (apical/basolateral) were calculated (Table II). At 20°C, relative lag times (apical/basolateral) were 30% longer (2-tail t test, P = 0.02) and relative rates (apical/basolateral) were 50% slower (P = 0.04) than at 37°C.

When CT was bound to T84 cell monolayers at 4°C and the cells were then warmed to 15°C (Fig. 5 *c* and Table II), the action of both apical and basolateral CT was completely inhibited, and Isc remained at baseline levels for the entire 400-min period monitored. The monolayers remained viable for the entire period at 15°C since re-warming above 32°C restored Cl^- secretion in all monolayers exposed initially to CT (peak Isc: 17 ± 1 and 13 ± 2 $\mu A/cm^2$; dIsc/dt: 0.31 ± 0.06 and 0.24 ± 0.02 $\mu A/cm^2/min$, apical and basolateral CT respectively, mean ± SE, n = 3). In agreement with our results at 37° and 20°C, the onset of Cl^- secretion after warm up from 15°C was significantly delayed for apical CT (50 ± 0.00 min apically vs. 35 ± 0.00 min basolaterally, 2-tail t test, P = 0.0001). In contrast, re-warming control monolayers not exposed to CT had no effect on Isc. To demonstrate the viability of these controls, 0.5 mM 8Br-cAMP was administered to serosal reservoirs and this was followed by a brisk secretory response (peak Isc, 16 ± 0.5 $\mu A/cm^2$; initial rate, 0.24 ± 0.01 $\mu A/cm^2/m$; mean ± SE, n = 3). In summary, these data show that lowering incubation temperatures to 20°C had a disproportionate effect on apical toxin action. Lowering incubation temperatures to 15°C, however, completely blocked the action of CT when applied to either pole of the cell.

Previous studies have shown that CT binds avidly to cell membranes at 4°C and will ribosylate $G_{\alpha s}$ and activate adenylate cyclase in isolated membrane preparations at this temperature (21). Reducing temperatures to 15°C did not by itself prevent Cl^- secretion since 8Br-cAMP rapidly (3–5 min) elicited a brisk secretory response at this temperature (initial rate: 0.79 ± 0.00 $\mu A/cm^2/min$; and peak Isc: 20.4 ± 0.8 $\mu A/cm^2$, mean ± SE, n = 6) (Fig. 6). Similarly, 15°C did not ablate basal activity of adenylate cyclase since 1 μM forskolin (Calbiochem-Behring Corp.) also elicited Cl^- secretion within 3 min at this temperature (initial rate: 0.8 ± 0.1 $\mu A/cm^2/min$; and peak Isc: 34 ± 4 $\mu A/cm^2$, mean ± SE, n = 6) (Fig. 6). Lastly, to demonstrate that reduced temperature had little effect on the time course of receptor-mediated signal transduction and activation of $G_{\alpha s}$, 1 nM vasoactive intestinal peptide (Calbiochem-Behring Corp.), was applied to serosal reservoirs of T84 monolayers at 15°C (Fig. 6) and again within 3 min, a strong Cl^- secretory response was observed (initial rate: 0.64 ± 0.06 $\mu A/cm^2/min$; and peak Isc: 32 ± 4 $\mu A/cm^2$, mean ± SE, n = 6). These results indicate that at 15°C, activation of $G_{\alpha s}$,

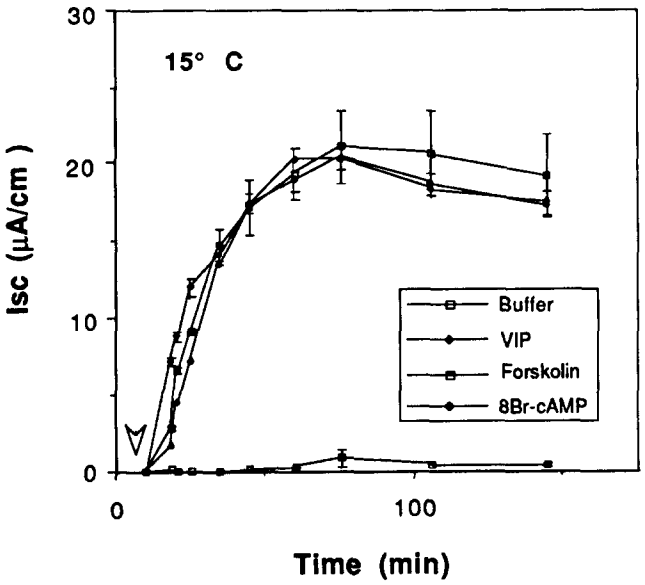

Figure 6. Time course of Cl^- secretion after administration of either 1 nM VIP, 1 μM forskolin, 3 mM 8Br-cAMP, or buffer alone to serosal reservoirs at 15°C (*open arrowhead*). Direct activation of $G_{\alpha s}$, adenylate cyclase, or protein kinase-A was not rate limiting at 15°C.

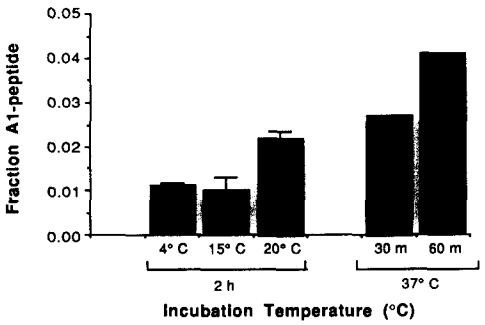

Figure 7. Temperature effect on reduction of apical ^{125}I-CT to the A_1-peptide by T84 cells. After 2 h at 15°C, the fraction of A-subunit reduced to the A_1-peptide was no different from background (4°C). At 20°C, the fraction reduced to the A_1-peptide was more than twofold greater than background (mean ± SE, n = 3; * ANOVA, $P < 0.006$) and was comparable to levels of A_1-peptide produced after 30 min at 37°C (30 and 60 min values at 37°C represent single independent measurements). Thus inhibition of apical toxin action at 20°C was not due to inhibition of generation of A_1-peptide.

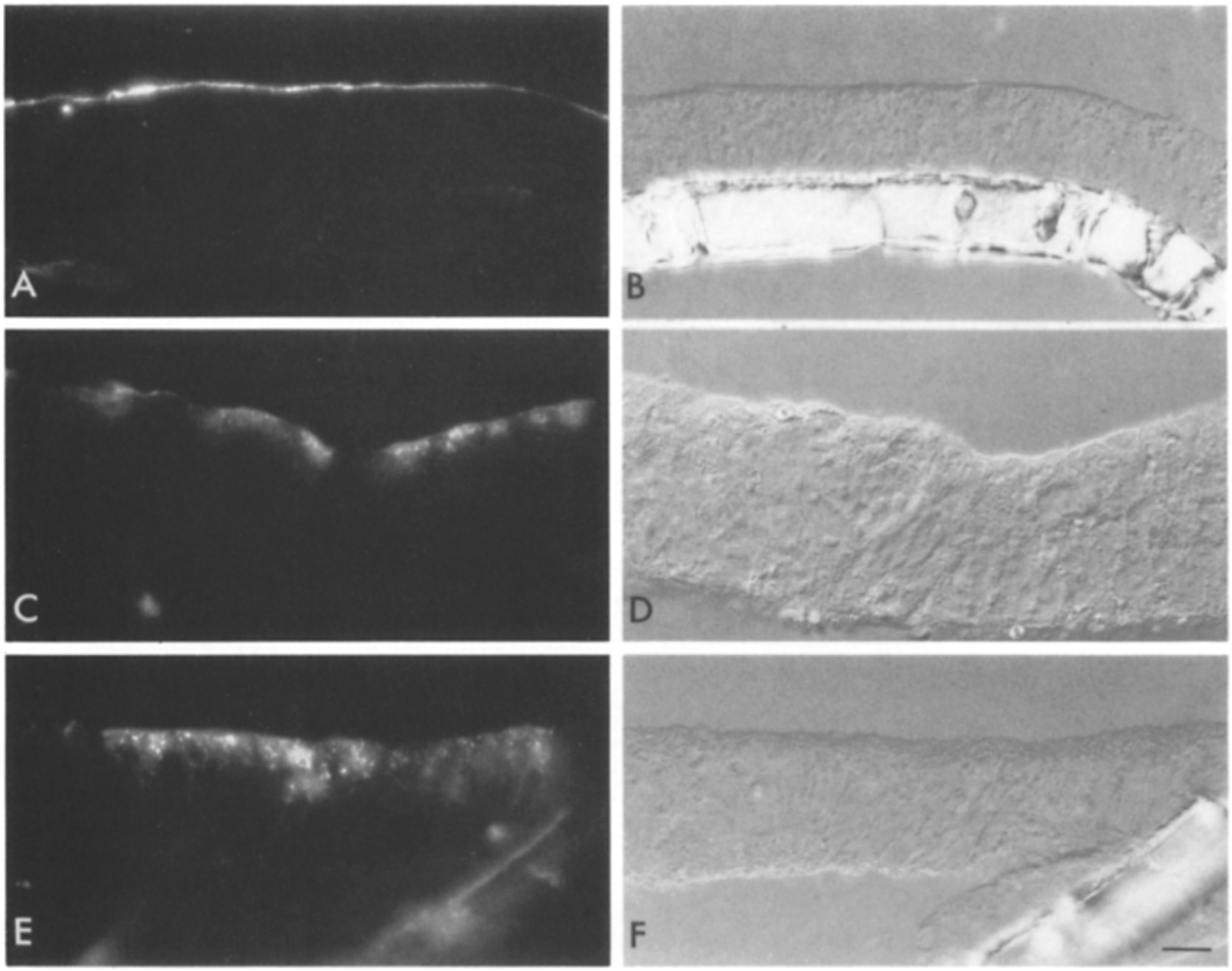

Figure 8. Epifluorescent and corresponding Nomarski micrographs of frozen 5-μm sections of T84 monolayers exposed apically to 20 nM rhodamine-labeled CT for 2 h at 4°C (*A* and *B*), 2 h at 20°C (*C* and *D*), or 1 h at 37°C (*E* and *F*). CT is internalized and located within apical structures at 20° and 37° but not at 4°C. Bar, 10 μm.

adenylate cyclase, or the cAMP-dependent Cl^- channel is not rate limiting.

A_1-peptide Is Generated from Apically Applied CT at 20°C

Available evidence indicates that cell-specific formation of the A_1-peptide occurs within the cytoplasm or as the A-subunit passes through the cell membrane (32, 35). For CT to act on any cell, the A-subunit must be reduced to the A_1-peptide during or after translocation across the membrane to the cytoplasmic membrane face, and this process is known to be time and temperature dependent (15, 35). Temperatures below 15°C have been shown to completely block translocation and formation of the A_1-peptide, and thus prevent CT action in several nonpolarized cell systems. Therefore, the differential effect of temperature on apical toxin-induced Cl^- secretion in polarized T84 cells at 20°C could possibly be accounted for by a temperature-dependent inhibition of A-subunit translocation across apical plasma membranes. To examine this possibility, we assessed the degree of reduction of CT to the A_1-peptide after application of toxin to apical membranes of T84 cells.

Radiolabeled ^{125}I-CT was preincubated with apical surfaces of T84 monolayers at 4°C for 30–60 min, and either kept at 4°C (controls) or warmed to 15°, 20°, or 37°C for an additional 120 min. Reduction of the A-subunit was detected by the appearance of radiolabeled A_1-peptide that is shifted in electrophoretic mobility on non-reducing polyacrylamide gels. Fig. 7 summarizes the results (mean ± SE, $n = 3$) of these experiments. As previously reported in nonpolarized cell systems (31, 35), the fraction of CT reduced to the A_1-peptide by T84 cells at 37°C was only a small fraction (2–5%) of total toxin bound. After 2 h at 15°C (a temperature which blocked the action of CT applied to either apical or basolateral cell surfaces), the fraction of reduced A_1-peptide remained at background levels (1.0 ± 0.3 vs. 1.1 ± 0.07%). Thus, the lack of response at 15°C may be entirely accounted for by the inability of the A-subunit to translocate across cell membranes at this temperature. In contrast, after 2 h at 20°C, a time that is well within the lag phase for apical and basolateral toxin at this temperature, apical CT was reduced and presumably translocated since the level of A_1-peptide was increased significantly (2.2 ± 0.1%; ANOVA, $P = 0.006$) and was comparable to levels attained

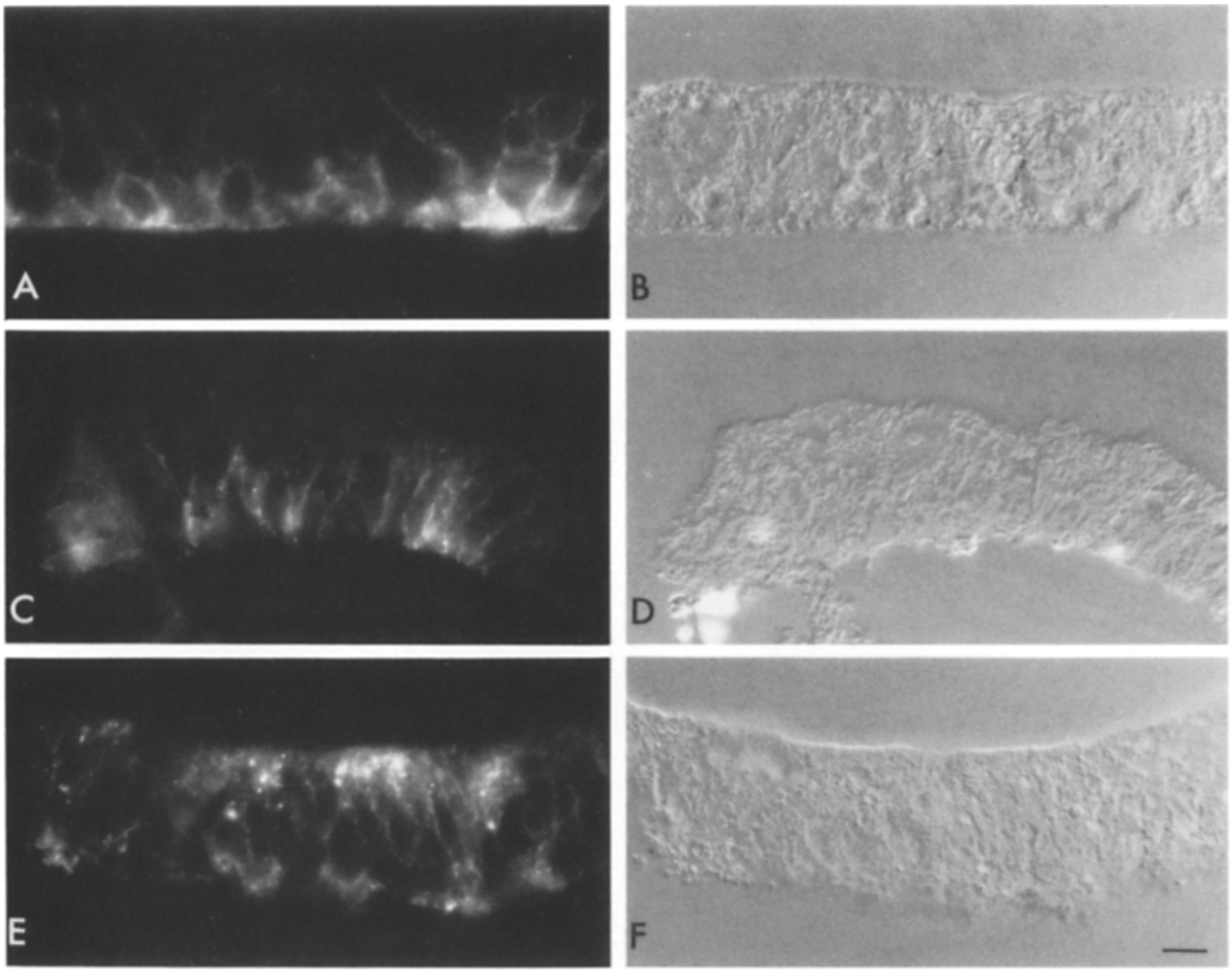

Figure 9. Epifluorescent and corresponding Nomarski micrographs of frozen 5-μm sections of T84 monolayers exposed basolaterally to 20 nM rhodamine-labeled CT (*CT-rhod*) for 2 h at 4°C (*A* and *B*), 2 h at 20°C (*C* and *D*), or 1 h at 37°C (*E* and *F*). CT is internalized and located within basolateral and apical structures at 37°C. Movement from basolateral surfaces to apical structures did not occur at 20°C. Bar, 10 μm.

after 30 min (2.7%, near the end of the lag phase) at 37°C. Generation of A_1-peptide, however, was not sufficient to cause Cl^- secretion in monolayers exposed to apical toxin at 20°C, since a secretory response was absent at 2 h and remained so for another 2 h. Thus, the stronger inhibition of apical CT action at 20°C can not be explained by the lack of membrane penetration or A-subunit reduction.

CT Is Endocytosed from Apical and Basolateral Surfaces of T84 Cells at 20°C

To examine endocytosis and vesicular transport of CT-containing membranes at different temperatures, CT was localized in T84 cells using a functional rhodamine-labeled toxin analogue (CT-rhod). CT-rhod elicited Cl^- secretion in T84 cells with an ED50 identical to that of native toxin (<0.5 nM, data not shown). After application of 20 nM CT-rhod to apical or basolateral surfaces at 4°C, CT-rhod outlined apical or basolateral cell membranes (Figs. 8 *a* and 9 *a*). Label was not apparent on the contralateral plasma membrane indicating that no detectable toxin passed through tight junctions. The intensity of apical or basolateral staining was not uniform among cells in a single monolayer, however, possibly indicating heterogeneity in number or accessibility of GM_1 sites within this T84 cell clone. As expected, fluorescence was not detected within intracellular structures at 4°C. Preincubation with 100-fold excess unlabeled CT eliminated the fluorescent signal entirely, indicating that the labeling was specific (data not shown).

After incubation with 20 nM apical CT-rhod at 20°C for 2 h (Fig. 8 *c*) or at 37°C for 1 h (Fig. 8 *e*), the rhodamine-labeled analogue was detected on apical cell surfaces and also within apically located structures, presumably endosomes. At 37°C for 1 h, internalization of the apical toxin analogue was more extensive, and CT was visualized in larger structures deeper in the apical cytoplasm, corresponding in position to late endosomes, lysosomes, and possibly Golgi. Movement of apical CT-rhod into basolateral regions, however, was not detected at either temperature. In monolayers exposed to CT basolaterally at 20°C for 2 h (Fig. 9 *c*), CT-rhod was visualized only at or near basolateral surfaces, corresponding in position to the basolateral membrane and possibly basolateral endosomes, as documented for other

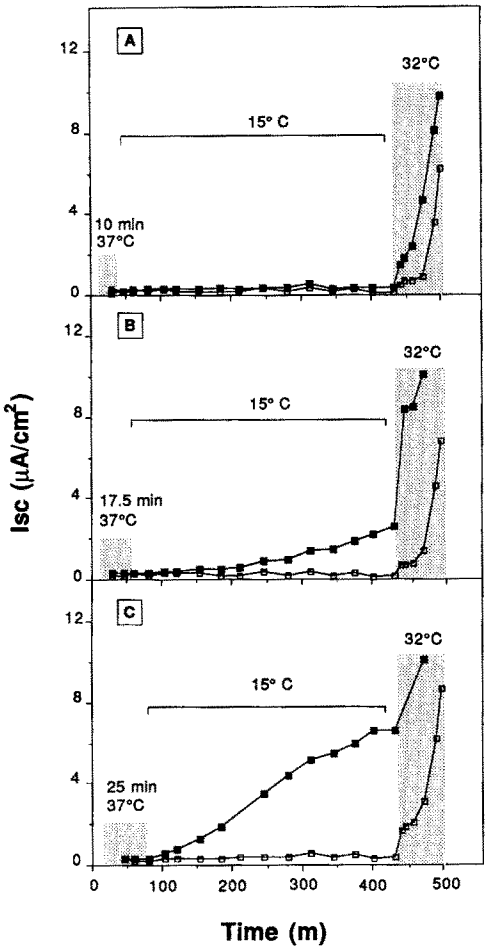

Figure 10. Temperature dependency of CT-induced Cl^- secretion after apical (*open squares*) and basolateral (*filled squares*) application of 120 nM CT at 4°C, priming at 37°C for 10 min (*A*), 17.5 min (*B*), or 25 min (*C*) and then returning to monolayers to 15°C. Shaded areas indicate the period in which the monolayers were warmed to 32°C. Priming the monolayers at 37°C for 17.5 and 25 min overcame the 15°C temperature block for basolateral but not apical CT. The length of the lag period for apical CT action after rewarming was inversely related to the duration of the initial 37° priming period (*A–C*). This can be appreciated graphically by comparing the sizes of the shaded areas beneath each curve defined by apical toxin (*open squares*).

tracers in previous studies (19). In contrast, 1 h after basolateral application at 37°C (Fig. 9 *e*), CT-rhod was detected in vesicular structures in both apical and basolateral regions of the cell, corresponding in position to late endosomes, lysosomes, and possibly Golgi. The data suggest that at both 20° and 37°C, T84 cells internalized CT into vesicular structures from either pole of the cell but vesicular transport beyond the apical or basolateral endosome was strongly inhibited at 20°C.

An Additional Temperature-dependent Event Is Required after Endocytosis of Apical CT and Generation of the A_1-Peptide

Having shown that formation of the A_1-peptide and endocytosis of CT-rhod occurred from the apical membrane at 20°C, at a time when Cl^- secretion had not begun, we

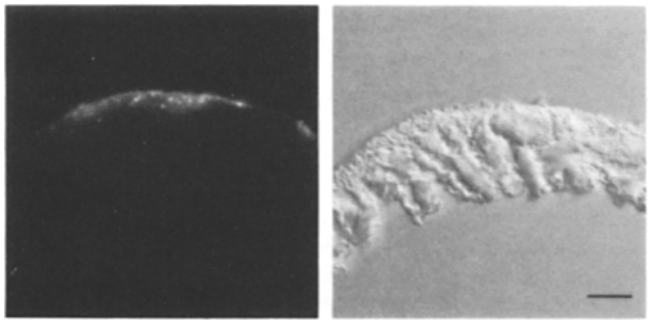

Figure 11. Epifluorescent and corresponding Nomarski micrographs of frozen 5-μm sections of T84 monolayers exposed apically to 20 nM rhodamine-labeled CT (*CT-rhod*) for 30 min at 4°C and subsequently warmed to 37°C for 25 min. At this time, CT has been internalized and is located within apical structures corresponding in position to apical endosomes. Bar, 10 μm.

sought to determine whether vesicular transport beyond the endosomal compartment plays a role in the secretory response. In all systems studied previously, vesicular transport beyond the endosome was effectively inhibited at temperatures below 20°C. In the CT-T84 cell system, incubation at 15°C completely blocked Cl^- secretion, but also blocked translocation of the A-subunit and formation of the A_1-peptide. Thus, no conclusions concerning vesicular transport could be drawn from the 15°C data.

To distinguish possible temperature effects due to vesicular transport from those due to toxin translocation, we applied CT to monolayers at 4°C, and then "primed" them by warming to 37°C for varying short periods (to allow endocytosis and A-subunit translocation) before returning them to a "nonpermissive" temperature. After exposure to CT apically or basolaterally at 4°C for 30 min, monolayers were shifted to 37°C for 10, 17.5, or 25 min and then returned to 15°C. Fig. 10 shows data from a representative experiment. When the cells were primed at 37°C for only 10 min, a time well within the lag periods defined above, the 15°C temperature block was not overcome; there was no response to CT applied to either pole of the cell (Fig. 10 *a*). In contrast, in monolayers warmed to 37°C for 17.5 (Fig. 10 *b*) or 25 min (Fig. 10 *c*), basolateral CT induced a Cl^- secretory response after a long lag period at 15°C, but the action of apical

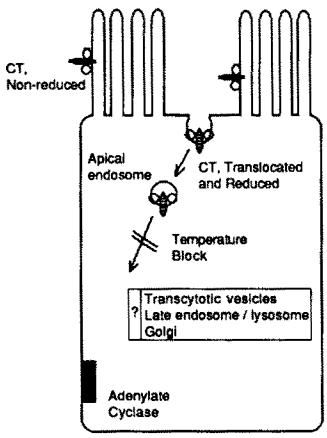

Figure 12. Proposed model for mechanism of CT action on polarized epithelia. Vesicular transport of CT-containing (or possibly $G_{\alpha s}$-containing) membranes allows apical CT to activate adenylate cyclase at the basolateral membrane.

CT was completely inhibited even after 400 min. Inhibition of secretion in the apically exposed monolayers was not due to epithelial cell damage at low temperature since rewarming to 32°C restored Cl^- secretion in all monolayers initially exposed to CT. The lag period that preceded toxin-induced Cl^- secretion in these monolayers after rewarming was inversely related to the duration of the initial 37° priming period (Fig. 10). Table II summarizes the results of seven independent experiments on monolayers primed at 37°C for 25 min and subsequently returned to the nonpermissive temperature of 15°C. Monolayers exposed to basolateral toxin responded with a Cl^- secretory response after a lag time of 105 ± 5.5 min, whereas Cl^- secretion was not detected in monolayers exposed to apical toxin, even after 400 min (the duration of the experiment). In one additional pair of monolayers primed for 30 min at 37°C before cooling to 15°C, the action of apical toxin was still completely inhibited, but a secretory response to basolateral toxin was clearly present (dIsc/dt = 0.06 $\mu A/cm^2/min$; lag = 89 min; peak Isc = 11.5 $\mu A/cm^2$). Previous experiments had shown that after 30 min at 37°C, the A_1-peptide has formed and the cells are near the end of the lag phase for apical toxin.

To provide direct evidence that apical CT had been endocytosed under these conditions, we examined by epifluorescence microscopy 5-μm frozen sections of T84 monolayers exposed apically to CT-rhod at 4°C and warmed to 37°C for 25 min before fixation. Fig. 11 shows that the fluorescent toxin analogue was present on apical cell surfaces and within vesicular structures close to the apical plasma membrane, but was not detected in deeper compartments at this time. Taken together, these data demonstrate that the ability of apical CT to induce Cl^- secretion requires a temperature-sensitive step that is not required when the toxin is applied to basolateral surfaces. This event occurs after entry of toxin into apical endosomes and after translocation and formation of the A_1-peptide. Our data suggest that the required event involves vesicular transport of toxin or possibly membrane-associated ADP-ribose $G_{\alpha s}$ to a site beyond the early apical endosomal compartment.

Discussion

In this report, we have defined T84 cells as a model for the study of CT action on intestinal epithelia and have used this model to show that intestinal epithelial cell polarity is an important factor in the mechanism of cholera-induced diarrhea. Our results identify an essential temperature-dependent step required for the action of apical (but not basolateral) CT on polarized cells. The data strongly support the hypothesis that this step includes vesicular transport of CT- or possibly $G_{\alpha s}$-containing membranes.

T84 Cells as a Model System to Study the Mechanism of CT Action

T84 cells grown as confluent monolayers have been well characterized as a model system for the study of regulated Cl^- secretion in intestinal epithelia (9). When grown on collagen-coated permeable supports, the cells form morphologically well-differentiated monolayers and express the necessary ion channels, symporters, and pumps in the appropriate membrane domains for vectorial transport of Cl^-. The ability of CT to elicit Cl^- secretion in T84 cells, however, has not been documented. This report demonstrates that T84 cells have all the necessary components for a physiologic response to CT, whether applied to apical or basolateral cell surfaces. After a distinct lag phase, CT induces a strong cAMP-dependent Cl^- secretory response from T84 monolayers that can be detected electrically with a high degree of temporal resolution. This system is particularly relevant for studies of the mechanism of CT action, because the response to CT in T84 cells reproduces the primary transport event of secretory diarrhea in humans.

Confluent monolayers of T84 cells form intercellular tight junctions with high transepithelial resistance (typically >1,000 ohms·cm^2), and well-defined charge and size selectivity (43). It has previously been shown that cAMP agonists do not influence solute permeation across T84 cell tight junctions (57) and thus the 84-kD CT molecule would not pass through tight junctions and would not gain access to the opposite cell surface by a paracellular route. Our serosal to mucosal Na^+ flux studies and our morphological data are consistent with this.

Effect of Epithelial Cell Polarity on the Mechanism of CT Action

CT bound to GM_1 in the apical plasma membrane of intestinal epithelial cells, cannot interact directly with adenylate cyclase in the basolateral membrane domain. This is in contrast to nonpolarized cells where CT can bind to membrane gangliosides in close proximity to the adenylate cyclase complex, and where transmembrane passage of A_1 to the cytosolic surface may be sufficient for toxin activity. Given the resemblance of epithelial basolateral membranes to membranes of nonpolarized cells (59), it may be predicted that the action of CT bound at the basolateral membrane of epithelial cells would be analogous to that of nonpolarized cells. Toxin bound at the apical surface, in contrast, must generate A_1-peptides that either travel through the cell themselves or ribosylate $G_{\alpha s}$ that in turn moves to the basolateral cyclase complex. In our studies, the effects of temperature on basolateral CT activity recapitulated exactly the temperature dependency of CT action exhibited by other nonpolarized cell systems (15), but the temperature dependency of apical CT did not. The longer lag phase, slower rate, and temperature sensitivity of Cl^- secretion due to apical CT suggested that the mechanism of toxin action is more complex in polarized epithelial cells.

Our data demonstrate that activation of adenylate cyclase by apical CT requires a temperature-sensitive step not required for toxin applied basolaterally to the same cells. The difference cannot be attributed to the effect of receptor density, as described in nonpolarized cells (18), because apical and basolateral toxin exhibited nearly identical dose dependency and apical and basolateral membranes of T84 cells apparently contain similar numbers of functional receptors. Furthermore, a difference between apical and basolateral membrane receptor numbers would not account for the dramatic effect of reduced temperature on apical toxin action after priming at 37°C for 25 or 30 min. Nor can our observations be explained by an exaggerated temperature effect on

the translocation of the A-subunit across the apical plasma membrane to the cell interior. Furthermore, we show that the processes of toxin translocation and reduction to the A_1-peptide did not fully account for the lag phase following toxin application to apical cell surfaces, and formation of the A_1-peptide alone was not sufficient for apical CT action. In contrast, in all nonpolarized cell systems previously studied, formation of the A_1-peptide corresponded closely to the onset of CT-action and accounted fully for the duration of the lag phase (28, 32, 35). Our studies are thus the first to demonstrate a dissociation between formation of the A_1-peptide and toxin action that is specific to polarized cells.

Role of Vesicular Membrane Transport in the Mechanism of CT Action

Endocytosis of CT has been demonstrated in both nonpolarized (34, 46) and polarized (25) cells. Direct evidence linking endocytosis with toxin activity, however, has only recently been obtained. Studies using membrane fractions of isolated hepatocytes exposed on the sinusoidal (basolateral) membrane to CT in vivo suggest that internalization of surface-bound toxin into acidic endosomes facilitates translocation of the A_1-peptide to the cytosolic membrane surface (32). The authors also propose that even from the hepatocyte basolateral membrane, vesicular transport of toxin-containing membranes is necessary for CT to gain access to $G_{\alpha s}$. In the case of polarized intestinal cells, a second hypothesis has been proposed based on the observation that rabbit intestinal brush border membranes contain $G_{\alpha s}$ (11). In this case, the authors suggest that CT catalyzes the ADP-ribosylation of $G_{\alpha s}$ within brush border membranes and that ADP-ribose-$G_{\alpha s}$ subsequently moves across the cell, by unknown mechanisms, to activate basolateral adenylate cyclase. The ability of any heterotrimeric GTPase to move to and activate effectors at distant sites, however, remains undocumented.

Although it has been argued that the A_1-peptide or ADP-ribose-$G_{\alpha s}$ (55) can break free of cell membranes to diffuse in the cytoplasm, inhibition of free diffusion could not explain our results. First, diffusion constants for macromolecules in aqueous solution are reduced only slightly when temperatures are lowered to 4°C (66). Although the temperature dependency for diffusion of molecules through cytosol has not been examined directly, reduced temperature tends to destabilize cytoskeletal structures, solate the cytoplasm (40), and enhance rather than inhibit the free diffusion of water soluble molecules as small as the A_1-peptide or ADP-ribose-$G_{\alpha s}$. Secondly, several lines of evidence from other systems indicate that the A_1-peptide does not diffuse freely in intact cells but remains membrane associated after translocation. The A_1-peptide is hydrophobic and when reconstituted into lipid vesicles behaves as an integral membrane protein (22, 23). In addition, when applied to intact fibroblasts, CT ribosylates only a specific subset of potential substrates suggesting that it does not have access to all cytoplasmic proteins (65). Whether activated $G_{\alpha s}$ breaks free of membranes to diffuse in the cytosol is controversial (1, 41, 55, 61), but it is now clear that the α-subunits of most other heterotrimeric GTPases remain membrane associated even after activation and dissociation from the $\beta\gamma$-dimer (14, 61). There is convincing data that $G_{\alpha s}$ also remains membrane associated after activation and that $G_{\alpha s}$ contains a 1-kD region at the carboxy terminus that is a putative site for membrane attachment (1). In our studies in intact cells, even after translocation of the A_1-peptide to the cytoplasmic side of the membrane, nonpermissive temperatures completely blocked the action of apical CT for almost 7 h. This strongly argues against the possibility that either the A_1-peptide or activated $G_{\alpha s}$ diffuse freely within the cytosol.

Our data may be best explained by a temperature effect on vesicular transport of membranes containing CT, or possibly $G_{\alpha s}$. By epifluorescence microscopy, we provided direct evidence that at 37°C the rhodamine-labeled toxin analogue was internalized into apical and basolateral endosomal compartments and transported to larger vesicular structures in the apical cytoplasm. These results are consistent with studies on MDCK cells (4, 63), Caco-2 cells (29), and native intestinal epithelia (19), which show that fluid phase or adsorbed tracer proteins enter separate early apical and basolateral endosomes, and are transported to common late endosomes and lysosomes located apically. At 20°C, in contrast, no transport of CT-rhod beyond apical or basolateral endosomes was observed in T84 cells. Transcellular movement or entry into Golgi compartments of a small but functionally significant fraction of apical toxin may have occurred at 37°C but would not have been visualized by our methods. The apparent lack of movement of apical CT to deeper vesicular structures or presumably to basolateral membrane compartments at 20°C was accompanied by inhibition or a complete block of apical toxin action. In other epithelial cell systems, temperatures of 20°C and below have been shown to block vesicular transport in the exocytic (30, 44), endosome–lysosome (13), and transcytotic pathways (5, 26). The molecular basis for low-temperature blocks of vesicular transport are still unknown (37), but reduced temperature could potentially affect vesicle budding, movement, or fusion with target membranes (2, 45). In intestinal cells, nonpermissive temperatures may block a membrane budding and/or fusion event necessary for the transport of the A_1-peptide, or possibly ADP-ribose-$G_{\alpha s}$, beyond early apical endosomes to basolateral structures that would allow access to the adenylate cyclase complex (Fig. 12). This event occurs after endocytosis of toxin containing membranes and after formation of the A_1-peptide. The data strongly support a role for vesicular membrane transport in the pathogenesis of CT-induced secretory diarrhea.

We thank Dennis Ausiello for critical reading of the manuscript and many helpful discussions.

This work was supported by National Institute of Health research grants DK21505, HD17557 (M. R. Neutra), DK35932, DK33506 (J. L. Madara) and Harvard Digestive Diseases Center grant DK34854. W. I. Lencer is recipient of Clinical Investigator Award KO8-DK01848 and a research grant from the Charles H. Hood Foundation.

Received for publication 27 December 1991 and in revised form 4 March 1992.

References

1. Audigier, Y., L. Journot, C. Pantaloni, and J. Bockaert. 1990. The carboxy-terminal domain of Gsα is necessary for anchorage of the activated form in the plasma membrane. *J. Cell Biol.* 111:1427–1435.

2. Balch, W. E., and J. E. Rothman. 1985. Characterization of protein transport between successive compartments of the golgi apparatus: asymmetric properties of donor and acceptor activities in a cell-free system. *Arch. Biochem. Biophys.* 240:413–425.
3. Bennett, V., and P. Cuatrecasas. 1975. Mechanism of action of *Vibrio cholerae* enterotoxin. *J. Membr. Biol.* 22:1–28.
4. Bomsel, M., K. Prydz, R. G. Parton, J. Gruenberg, and K. Simons. 1989. Endocytosis in filter-grown Madin-Darby canine kidney cells. *J. Cell Biol.* 109:3242–3258.
5. Brandli, A. W., R. G. Parton, and K. Simons. 1990. Transcytosis in MDCK cells: identification of glycoproteins transported bidirectionally between both plasma membrane domains. *J. Cell Biol.* 111:2902–2921.
6. Cassel, D., and Z. Selinger. 1977. Mechanism of adenylate cyclase activation by cholera toxin: inhibition of GTP hydrolysis at the regulatory site. *Proc. Natl. Acad. Sci. USA.* 74:3307–3311.
7. Cassuto, J., M. Jodal, and O. Lundgren. 1981. On the role of intramural nerves in the pathogenesis of cholera toxin-induced intestinal secretion. *Scand. J. Gastroent.* 16:377–384.
8. Cuatrecasis, P. 1973. Gangliosides and membrane receptors for cholera toxin. *Biochemistry.* 12:3558–3566.
9. Dharmsathaphorn, K., and J. L. Madara. 1990. Established intestinal cell lines as model systems for electrolyte transport studies. *Methods Enzymol.* 192:354–359.
10. Dominguez, P., F. Barros, and P. S. Lazo. 1985. The activation of adenylate cyclase from small intestinal epithelium by cholera toxin. *Eur. J. Biochem.* 146:533–538.
11. Dominguez, P., G. Velasco, F. Barros, and P. S. Lazo. 1987. Intestinal brush border membranes contain regulatory subunits of adenyl cyclase. *Proc. Natl. Acad. Sci. USA.* 84:6965–6969.
12. Donowitz, M., and M. J. Welsh. 1987. Regulation of mammalian small intestinal electrolyte secretion. *In* Physiology of the Gastrointestinal Tract. J. R. Johnson, editor. Raven Press, New York. 1351–1388.
13. Dunn, W. A., A. L. Hubbard, and N. N. Aronson. 1980. Low temperature selectively inhibits fusion between pinocytic vesicles and lysosomes during heterophagy of ^{125}I-asialofetuin by the perfused rat liver. *J. Biol. Chem.* 255:5971–5978.
14. Eide, B., P. Gierschik, G. Milligan, I. Mullaney, C. Unson, P. Goldsmith, and A. Spiegel. 1987. GTP-binding proteins in brain and neutrophil are tethered to the plasma membrane via their amino termini. *Biochem. Biophys. Res. Commun.* 148:1398–1405.
15. Fishman, P. H. 1980. Mechanism of action of cholera toxin: studies on the lag period. *J. Membr. Biol.* 54:61–72.
16. Fishman, P. H. 1982. Internalization and degradation of cholera toxin by cultured cells: relationship to toxin action. *J. Cell Biol.* 93:860–865.
17. Fishman, P. H. 1982. Role of membrane gangliosides in binding and action of bacterial toxins. *J. Memb. Biol.* 69:85–97.
18. Fishman, P. H., and E. E. Stikkaw. 1980. Mechanism of action of cholera toxin: Effect of receptor density and multivalent binding on activation of adenylate cyclase. *J. Membr. Biol.* 54:51–60.
19. Fujita, M., F. Reinhart, and M. Neutra. 1990. Convergence of apical and basolateral endocytic pathways at apical late endosomes in absorptive cells of suckling rat ileum *in vivo*. *J. Cell Sci.* 97:385–394.
20. Gill, D. M., and R. Meren. 1978. ADP-ribosylation of membrane proteins catalysed by cholera toxin: basis of the activation of adenylate cyclase. *Proc. Natl. Acad. Sci. USA.* 75:3050–3054.
21. Gill, M. 1976. Multiple role of erythrocyte supernatant in the activation of adenylate cyclase by *Vibrio cholerae* toxin in vitro. *J. Infect. Dis.* 133:S55–S63.
22. Goins, B., and E. Freire. 1985. Lipid phase separations by the association of Cholera toxin to phospholipid membranes containing ganglioside GM1. *Biochemistry.* 24:1791–1797.
23. Goins, B., and E. Freire. 1988. Thermal stability and intersubunit interactions of cholera toxin in solution and in association with its cell-surface receptor ganglioside G_{M1}. *Biochemistry.* 27:2046–2052.
24. Halm, D. R., and R. A. Frizzell. 1990. Intestinal chloride secretion. *In* Textbook of Secretory Diarrhea. E. Lebenthal and M. E. Duffey, editors. Raven Press, New York. 47–58.
25. Hansson, H.-A., S. Lange, and I. Lonnroth. 1984. Internalization in vivo of cholera toxin in the small intestinal epithelium of the rat. *Acta. Pathol. Microbiol. Scand.* 92:15–21.
26. Herzog, V. 1983. Transcytosis in thyroid follicle cells. *J. Cell Biol.* 97:607–617.
27. Holmgren, J., I. Lonnroth, J.-E. Mansson, and L. Svennerholm. 1975. Interaction of cholera toxin and membrane ganglioside of small intestine. *Proc. Natl. Acad. Sci. USA.* 72:2520–2524.
28. Hughes, R. J., and P. A. Insel. 1983. Human platelets are defective in processing of cholera toxin. *Biochem. J.* 212;669–678.
29. Hughson, E. J., and C. R. Hopkins. 1990. Endocytic pathways in polarized Caco-2 cells: identification of an endosomal compartment accessible from both apical and basolateral surfaces. *J. Cell Biol.* 110:337–348.
30. Jamieson, J. D., and G. E. Palade. 1968. Intracellular transport of secretory proteins in the pancreatic exocrine cell. *J. Cell Biol.* 39:589–603.
31. Janicot, M., J.-P. Clot, and B. Desbuquois. 1988. Interactions of cholera toxin with isolated hepatocytes—Effects of low pH, chloroquine and monensin on toxin internalization, processing and action. *Biochem. J.* 253:735–743.
32. Janicot, M., F. Fouque, and B. Desbuquois. 1991. Activation of rat liver adenylate cyclase by cholera toxin requires toxin internalization and processing in endosomes. *J. Biol. Chem.* 266:12858–12865.
33. Johnson, G. L., H. R. Kaslow, and H. R. Bourne. 1978. Genetic evidence that cholera toxin substrates are regulatory components of adenylate cyclase. *J. Biol. Chem.* 253:7120–7123.
34. Joseph, K. C., A. Stieber, and N. K. Gonatas. 1979. Endocytosis of cholera toxin in GERL-like structures of murine neuroblastoma cells pretreated with GM1 ganglioside. *J. Cell Biol.* 81:543–554.
35. Kassis, S., J. Hagmann, P. H. Fishman, P. P. Chang, and J. J. Moss. 1982. Mechanism of action of cholera toxin on intact cells: generation of A1 peptide and activation of adenylate cyclase. *J. Biol. Chem.* 257:12148–12152.
36. Kimberg, D. V., M. Field, J. Johnson, A. Henderson, and E. Gershon. 1971. Stimulation of intestinal adenyl cyclase by cholera enterotoxin and prostaglandins. *J. Clin. Invest.* 50:1218–1230.
37. Kuismanen, E., and J. Saraste. 1989. Low temperature-induced transport blocks as tools to manipulate membrane traffic. *Methods Cell Biol.* 32: 257–274.
38. Lencer, W. I., S. H. Chu, and W. A. Walker. 1987. Differential binding kinetics of cholera toxin to developing intestinal microvillus membrane. *Infect. Immun.* 55:3126–3130.
39. LoSpalluto, J. J., and R. A. Finkelstein. 1972. Chemical and physical properties of cholera exo-enterotoxin (choleragen) and its spontaneously formed toxoid (Choleragenoid). *Biochim. Biophys. Acta.* 257:158–166.
40. Luby-Phelps, K., F. Lanni, and D. L. Taylor. 1988. The submicroscopic properties of cytoplasm as a determinant of cellular function. *Annu. Rev. Biophys. Biophys. Chem.* 17:369–396.
41. Lynch, C. J., L. Morbach, P. F. Blackmore, and J. H. Exton. 1986. α-Subunits of N_S are released from the plasma membrane following cholera toxin activation. *FEBS (Fed. Eur. Biochem. Soc.) Lett.* 200:333–336.
42. Madara, J. L., and K. Dharmsathaphorn. 1985. Occluding junction structure-function relationships in a cultured epithelial monolayer. *J. Cell Biol.* 101:2124–2133.
43. Madara, J. L., S. Colgan, A. Nusrat, C. Delp, and C. Parkos. 1991. A simple approach to measurement of electrical parameters of cultured epithelial monolayers. *J. Tiss. Cult. Tech.* In press.
44. Matlin, K. S., and K. Simons. 1983. Reduced temperature prevents transfer of a membrane glycoprotein to the cell surface but does not prevent terminal glycosylation. *Cell.* 34:233–243.
45. Mayorga, L. S., R. Diaz, and P. D. Stahl. 1989. Reconstitution of intracellular vesicle fusion in a cell-free system after receptor-mediated endocytosis. *Methods Cell Biol.* 32:179–196.
46. Montesanto, R., J. Roth, and L. Orci. 1982. Non-coated membrane invaginations are involved in binding and internalization of cholera and tetanus toxins. *Nature (Lond.).* 296:651–653.
47. Moore, R., C. Pothoulakis, J. T. Lamont, S. Carlson, and J. L. Madara. 1990. *C. difficile* toxin A increases intestinal permeability and induces Cl^- secretion. *Am. J. Physiol.* 259:G165–G172.
48. Moss, J., and M. Vaughan. 1977. Mechanism of action of choleragen: evidence for ADP-ribosyltransferase activity with arginine as an acceptor. *J. Biol. Chem.* 252:2455–2457.
49. Murer, H., E. Ammann, J. Biber, and U. Hopfer. 1976. The surface membrane of the small intestinal epithelial cell—Localization of adenyl cyclase. *Biochim. Biophys. Acta.* 433:509–519.
50. Parkinson, D. K., H. Ebel, D. R. DiBona, and G. W. G. Sharp. 1972. Localization of the action of cholera toxin on adenyl cyclase in mucosal epithelial cells of rabbit intestine. *J. Clin. Invest.* 51:2292–2298.
51. Parkos, C. A., C. Delp, M. A. Arnaout, and J. L. Madara. 1991. Neutrophile migration across a cultured intestinal epithelium: dependence on a CD11b/CD18-mediated event and enhanced efficiency in physiological direction. *J. Clin. Invest.* 88:1605–1612.
52. Peterson, J. W., and L. G. Ochoa. 1989. Role of prostaglandins and cAMP in the secretory effects of cholera toxin. *Science (Wash. DC).* 245:857–859.
53. Peterson, J. W., J. J. LoSpalluto, and R. A. Finkelstein. 1972. Localization of cholera toxin in vivo. *J. Infect. Dis.* 126:617–628.
54. Quill, H., and M. M. Weiser. 1975. Adenylate and guanylate cyclase activities and cellular differentiation in rat small intestine. *Gastroenterology.* 69:470–478.
55. Ransnas, L. A., P. Svoboda, J. R. Jasper, and P. A. Insel. 1989. Stimulation of B-adrenergic receptors of S49 lymphoma cells redistributes the α subunit of the stimulatory G protein between cytosol and membranes. *Proc. Natl. Acad. Sci. USA.* 86:7900–7903.
56. Ribi, H. O., D. S. Ludwig, K. L. Mercer, G. K. Skoolnik, and R. D. Kornberg. 1988. Three dimensional structure of cholera toxin penetrating a lipid membrane. *Science (Wash. DC).* 239:1272–1276.
57. Shapiro, M., J. Matthews, G. Hecht, C. Delp, and J. L. Madara. 1991. Stabilization of F-actin prevents cAMP elicited Cl secretion in T84 cells. *J. Clin. Invest.* 87:1903–1909.
58. Sharp, G. W. G., and S. Hynie. 1971. Stimulation of intestinal adenyl cy-

clase by cholera toxin. *Nature (Lond.).* 229:266–269.
59. Simons, K., and A. Wandinger-Ness. 1990. Polarized sorting in epithelia. *Cell.* 62:207–210.
60. Sixma, T. K., S. E. Pronk, H. H. Kalk, E. S. Wartna, B. A. M. van Zanten, B. Witholt, and W. G. J. Hol. 1991. Crystal structure of a cholera toxin-related heat-labile enterotoxin from E. coli. *Nature (Lond.).* 351:371–377.
61. Spiegel, A. M., P. S. Backlund, J. E. Butrynski, T. L. Z. Jones, and W. F. Simonds. 1991. The G protein connection: molecular basis of membrane association. *Trends Biol. Sci.* 16:338–341.
62. Spiegel, S., R. Blumenthal, P. Fishman, and J. S. Handler. 1985. Gangliosides do not move from apical to basolateral plasma membrane in cultured epithelial cells. *Biochim. Biophys. Acta.* 821:310–318.
63. Van Deurs, B., S. H. Hansen, O. W. Petersen, E. Lokhen-Melby, and K. Sandvig. 1990. Endocytosis, intracellular transport and transcytosis of the toxic protein ricin by a polarized epithelium. *Eur. J. Cell Biol.* 51:96–109.
64. Walling, M. W., A. K. Mircheff, C. H. Van Os, and E. M. Wright. 1978. Subcellular distribution of nucleotide cyclases in rat intestinal epithelium. *Am. J. Physiol.* 235:E539–E545.
65. Watkins, P. A., J. Moss, and M. Vaughan. 1981. ADP ribosylation of membrane proteins from human fibroblasts: effect of prior exposure of cell to choleragen. *J. Biol. Chem.* 256:4895–4899.
66. Weast, R. C. 1967. Viscosity. *In* Handbook of Chemistry and Physics. R. C. Weast, editor. The Chemical Rubber Co., Cleveland, OH. F33.
67. Wisnieski, B. J., and J. S. Bramhall. 1981. Photolabeling of cholera toxin subunits during membrane penetration. *Nature (Lond.).* 289:319–321.